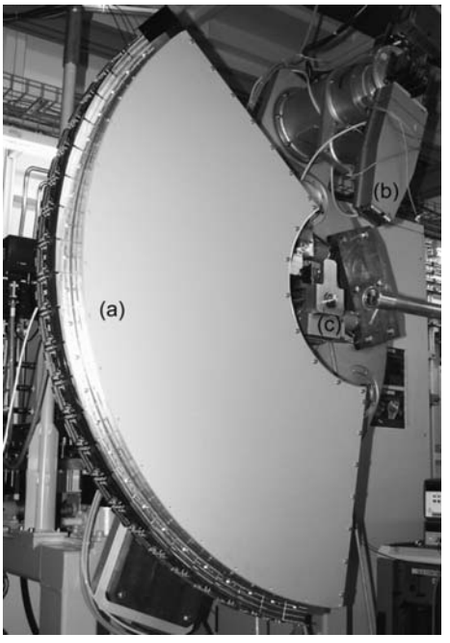

Figure 2.2.13
(*a*) 120° Mythen detector box, containing helium, mounted on the powder diffractometer of the materials science beamline at the Swiss Light Source. (*b*) Multianalyser detector stage. (*c*) Capillary spinner. (Bergamaschi *et al.*, 2009, 2010.)

background. The detector arm is scanned and a powder pattern recorded. This arrangement can be used for narrow capillary samples on lower-flux sources, avoiding the loss of intensity that use of an analyser crystal entails. The resolution is largely determined by the opening angle defined by the capillary and the receiving slit. Despite the simplicity of such an instrument, high-quality high-resolution data can be obtained.

For much faster data acquisition, a one-dimensional (1D) PSD or an area detector can be employed. Any sort of 1D detector with an appropriate number of channels, channel separation, efficiency, count rate (in an individual channel and overall) and speed of read out can be employed. Technology evolves and detectors make continual progress in performance. At the time of writing the most advanced 1D detector is the Mythen module developed by the Swiss Light Source (SLS). Mythen modules are based on semiconducting silicon technology and have 1280 8-mm-wide strips with a 50 µm pitch (64 × 8 mm^2). They can be combined to form very large curved detectors such as that on the powder diffractometer of the materials science beamline at the SLS (Fig. 2.2.13). This detector consists of 24 modules, 30 720 channels, set on a radius of 760 mm, covering 120° 2θ. Detector elements are therefore separated by ∼0.004°. The whole detector can be read out in 250 µs. Being Si based, its efficiency falls off above 20–25 keV, where the absorbing power of Si falls to very small values. Nevertheless, at intermediate and low energies a full powder-diffraction pattern for structural analysis can be measured in just seconds, or even faster if the intention is to follow a dynamic process.

Two-dimensional (2D) detectors are generally flat, so cannot extend to the same 2θ values as a curved multistrip detector unless scanned on a detector arm. This is possible, but usually a short wavelength is used with a fixed detector. This allows an adequate data range to be recorded, particularly if the detector is positioned with the direct beam (2θ = 0) near an edge. A 2D detector records complete or partial Debye–Scherrer rings, which increases the counting efficiency with respect to scanning an analyser crystal by several orders of magnitude. In addition, if the rings do not appear smooth and homogeneous, this indicates problems with the sample, such as preferred orientation or granularity, both of which can seriously affect diffraction intensities when measuring just a thin vertical strip. Detectors that have been used are diverse and include image plates, though these have slow read out, charge-coupled devices (CCDs) or Si-based photon-counting pixel detectors used for single-crystal diffraction or protein crystallography (*e.g.* Broennimann *et al.*, 2006), and medical-imaging detectors, which are designed for hard-energy operation. Examples include the CCD-based Frelon camera, developed at the ESRF (Labiche *et al.*, 2007), and commercially available large flat-panel medical-imaging detectors up to 41 × 41 cm^2, based on scintillator-coated amorphous silicon, which have been exploited at speeds of up to 60 Hz for selected read-out areas (Chupas, Chapman & Lee, 2007; Lee, Aydiner *et al.*, 2008; Daniels & Drakopoulos, 2009).

Note that a 2D detector can be used as a 1D detector by applying a mask and reading out only a narrow strip, which can enhance the rate of data acquisition. For CCD chips, the electronic image can be rapidly transferred to pixels behind the masked part of the detector from where it can be read out while the active area is re-exposed. Translating an image plate behind a mask is a simple way of acquiring a series of diffraction patterns for following a process with modest time resolution.

These instruments are vulnerable to aberrations that cause systematic shifts in peak positions, such as misalignment of the capillary or surface of the sample from the diffractometer axis, and specimen transparency, which also affects the peak width and shape. The peak width also depends on whether a flat sample is in the $\theta/2\theta$ condition, or on the diameter of a capillary sample, *etc*. Focusing the incident beam onto the detector decreases the peak width, as fewer pixels are illuminated compared to using a highly collimated incident beam. PSDs are much more open detectors than those behind an analyser crystal or set of slits, so are more susceptible to background and parasitic scatter from sample environments *etc*. However, the speed and efficiency of data acquisition usually outweigh such concerns.

2.2.4.3. *Energy-dispersive instruments*

The broad, continuous spectrum from a wiggler or bending magnet is suitable for energy-dispersive diffraction (EDD). Here, the detector is fixed at an angle 2θ and the detector determines the energy, ε, of each arriving photon scattered by the sample (Fig. 2.2.14). The energy [keV] can be converted to *d*-spacing [Å] *via*

$$d \simeq 12.3984/2\varepsilon \sin\theta.$$

The detector usually consists of a cryogenically cooled semiconducting Ge diode. An absorbed X-ray photon promotes electrons to the conduction band in proportion to its energy. By

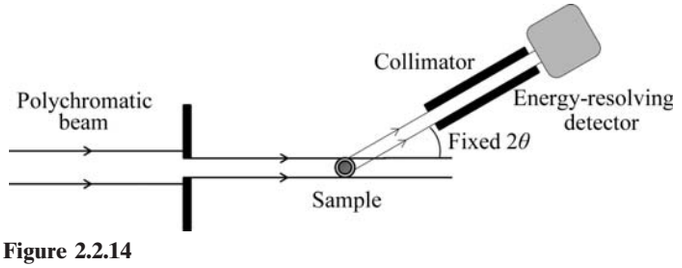

Figure 2.2.14
Schematic representation of an energy-dispersive diffraction arrangement.

analysing the size of the charge pulse produced, the energy of the photon is determined. The powder-diffraction pattern is recorded as a function of energy (typically somewhere within the range 10–150 keV, depending on the source) *via* a multichannel analyser (MCA). Instruments may have multiple detectors, at different 2θ angles covering different ranges in d-spacing (Barnes *et al.*, 1998), or arranged around a Debye–Scherrer ring, as in the 23-element semi-annular detector at beamline I12 at Diamond Light Source (Korsunsky *et al.*, 2010; Rowles *et al.*, 2012).

Prior to performing the EDD experiment, the detector and MCA system must be calibrated, *e.g.* by measuring signals from sources of known energy, such as ^{241}Am (59.5412 keV) or ^{57}Co (122.06014 and 136.4743 keV) at hard energies, and/or from the fluorescence lines of elements such as Mo, Ag, Ba *etc*. The 2θ angle also needs to be calibrated if accurate d-spacings are desired. This should be done by measuring the diffraction pattern of a standard sample with known d values.

The detector angle is typically chosen in the range 2–6° 2θ and influences the range of d-spacings accessible *via* the term $1/\sin\theta$, *i.e.* the lower the angle, the higher the energy needed to access any particular d. Normally, the range of most interest should be matched to the incident spectrum, taking account also of sample absorption and fluorescence, to produce peaks with high intensity. More than one detector at different angles can also be employed. Energy-sensitive Ge detectors do not count particularly fast, up to 50 kHz being a typical value compared to possibly 1–2 MHz with a scintillation detector. Hence they are relatively sensitive to pulse pile-up and other effects of high count rates (Cousins, 1994; Laundy & Collins, 2003; Honkimäki & Suortti, 2007), particularly if the synchrotron is operating in a mode with a few large electron bunches giving very intense pulses of X-rays on the sample.

The energy resolution of the detector is of the order of 2%, which dominates the overall resolution of the technique. Its main uses are where a fixed geometry with penetrating X-rays is required, *e.g.* in high-pressure cells, for *in situ* studies (Häusermann & Barnes, 1992), *e.g.* of chemical reactions under hydrothermal conditions (Walton & O'Hare, 2000; Evans *et al.*, 1995), electrochemistry (*e.g.* Scarlett *et al.*, 2009; Rijssenbeek *et al.*, 2011; Rowles *et al.*, 2012), or measurements of residual strain (Korsunsky *et al.*, 2010). Owing to the use of polychromatic radiation, the technique has very high flux on the sample and can be used for high-speed data collection, following rapid processes *in situ*. However, accurate modelling of the intensities of the powder-diffraction pattern for structural or phase analysis is difficult because of the need to take several energy-dependent effects into account, *e.g.* absorption and scattering factors, the incident X-ray spectrum, and the detector response. Nevertheless, examples where this has been successfully carried out have been published (*e.g.* Yamanaka & Ogata, 1991; Scarlett *et al.*, 2009).

A higher-resolution variant of the energy-dispersive technique can be performed by using a standard detector behind a collimator at fixed 2θ scanning the incident energy *via* the monochromator. The Hart–Parrish design with long parallel foils is suitable. Such an approach has been demonstrated in principle (Parrish, 1988), but is rarely used in practice. The advantage is to be able to measure data of improved d-spacing resolution, as compared to using an energy-dispersive detector, from sample environments with highly restricted access. In principle, as a further variant, white incident radiation could be used with scanning of θ_a, the angle of the analyser crystal, and associated detector at $2\theta_a$, all at fixed 2θ.

2.2.5. Considerations for powder-diffraction experiments

Synchrotron radiation allows considerable flexibility for a powder-diffraction experiment, offering choice and optimization of a number of quantities such as the wavelength, with high energy resolution, range in d-spacing, angular resolution, angular accuracy, and spatial or time resolution (but not all of these can necessarily be optimized at the same time). Increasingly, powder-diffraction experiments at synchrotrons are combined with complementary measurements, simultaneously applying techniques such as Raman spectroscopy (Boccaleri *et al.*, 2007; Newton & van Beek, 2010), particularly when carrying out *in situ* studies of an evolving system. In this respect, the open nature of a synchrotron instrument, with space around the sample to position auxiliary equipment, is an advantage.

2.2.5.1. *Polarization*

Assuming the beam is 100% polarized in the horizontal plane of the synchrotron orbit and with detection in the vertical plane, there is no need for any polarization correction to the diffracted intensities. However, if a small amount of vertical polarization of the beam does need to be taken into account (possibly up to a few per cent depending on the source), the polarization factor that describes its effect on the intensity of the diffracted beam can be derived, following the approach of Azároff (1955) and Yao & Jinno (1982), as

$$P = \frac{1 - dp + dp\cos^2 2\theta\cos^2 2\theta_a}{1 - dp + dp\cos^2 2\theta_a} = \frac{1 - dp + dp\cos^2 2\theta\cos^2 2\theta_a}{1 - dp\sin^2 2\theta_a}, \tag{2.2.3}$$

where dp is the depolarization fraction (*i.e.* the fraction of the total intensity incident on the sample that is vertically polarized), $2\theta_a$ is the Bragg angle of the analyser crystal (if any), and the denominator scales P to unity at 2θ equal to zero (Dwiggins, 1983) and is a constant for any particular experimental setup. If there is no analyser crystal, or we ignore the effect it would have (*i.e.* by putting $2\theta_a = 0$), then

$$P = 1 - dp\sin^2 2\theta.$$

Beamline staff can usually advise on the appropriate values to use. These expressions reduce to the usual polarization factor for unpolarized (dp = 0.5) laboratory X-rays without a monochromator or analyser crystal, $\frac{1}{2}(1 + \cos^2 2\theta)$.

An alternative formulation of equation (2.2.3) considers the ratio of the vertical to horizontal polarization,

$$rp = \frac{dp}{1 - dp} \quad \text{and} \quad dp = \frac{rp}{1 + rp},$$

so that

$$P = \frac{1 + rp\cos^2 2\theta\cos^2 2\theta_a}{1 + rp\cos^2\theta_a}. \tag{2.2.4}$$

Note that rp = 1.0 for unpolarized (laboratory) X-rays. In reality, because the synchrotron beam is near 100% plane polarized, dp and rp have similar values. The same expressions can be used if diffracting and analysing in the horizontal plane, except that now the value of dp or rp is replaced with the value of $(1 - dp)$ or $1/rp$, respectively.

For Debye–Scherrer rings detected on a 2D detector, the azimuthal angle around the ring needs to be taken into account, yielding